Implementing CFD Modelling to Address Defect Formation in Core Injection Moulding

Stefano Cademartori, Nicholas Humphreys, Jean-Christophe Gebelin and Jeffery Brooks

Abstract Ceramic cores are used in casting processes to create complex internal shapes within the final component. The work presented here uses Computational Fluid Dynamics (CFD) analysis to predict the filling and solidification behaviour of ceramic core material during the Ceramic Injection Moulding (CIM) process in the large, complex geometries now typical of modern cores. The aim of the study is to develop a predictive capability to identify key defects in the core that might otherwise only be observed after a number of expensive manufacturing processes. Manufacturing trials using short shots have been carried out in order to validate the transient flow patterns of the paste; this has highlighted the occurrence of jetting, weld lines and flow defects that are highly dependent on the injection parameters and runner designs employed. Analysis of the modelled solidification, shear rates, stagnation points and phase migration has driven die and process optimisation in a production environment.

Keywords CIM · Injection moulding · CFD · Process · Simulation Ceramic · Defect · StarCCM+

Introduction

High working temperatures increase the efficiency of gas-turbines engines, therefore modern components are designed for extreme operating conditions, even beyond the melting temperature of the alloy. Flowing cooling air within and across the surfaces of the components, or film cooling, is one of the technologies used to cool down the turbine blades and vanes [1]. The geometry of the channels is usually complex to increase turbulence and surface area for heat exchange. To achieve such

S. Cademartori (✉) · J. Brooks
University of Birmingham, Edgbaston, Birmingham, B15 2TT, United Kingdom
e-mail: stefano.cademartori@gmail.com

N. Humphreys · J.-C. Gebelin
Doncasters Group, Innovation House, Droitwich, WR9 9RB, United Kingdom

L. Nastac et al. (eds.), *CFD Modeling and Simulation in Materials Processing 2018*, The Minerals, Metals & Materials Series,
https://doi.org/10.1007/978-3-319-72059-3_20

degree of complexity, metal is cast around ceramic cores housed inside investment moulds. The cores are then removed via chemical etching [2].

The shape complexity, the high production volume and the surface quality required in the production of cores, make injection moulding the most frequently used forming technique for this purpose. However, the selection of the process parameters, often found empirically, makes the process challenging to set up and not suitable for small production runs. The core material is formed of ceramic powders, mixed with a suitable wax binder system, which promotes an even distribution of the powder while injected into a mould. The binder also allows compaction of the powder to form a so-called 'green body', which is heated in a furnace for de-binding, and then sintering [2].

If the selection of injection parameters or paste formulation is poor, it can lead to the formation of defects, that may only be detectable after costly thermal treatments (the most time consuming and energy expensive steps of the process) [2, 3]. Moreover, to inject sound cores, the dies used in CIM require high wear resistance, fluid cooling channels, gas vents and an ejection system to extract the solid core. Despite the consequential high up-front cost of tooling, the dies are not commonly designed accounting for the behaviour of the fluid material during injection.

The implementation of a mathematical model able to predict defect formation in the production of complex CIM parts opens the possibility for engineers to design dies specifically for the injected material, shifting from a tool-maker die design to a process oriented die design. Furthermore, the understanding of the injection conditions enables the optimisation of machine parameters in order to reduce production problems with existing moulds.

This work reports some of the insight on defect formation achieved through modelling of a number of core geometries, injection profiles and material systems. Due to the strictly confidential origin of the work neither material data nor detailed pictures will be given.

Materials and Methods

The core materials injected into the die are highly loaded ceramic wax systems. These ceramic pastes must be able to achieve a complex shape, fine surface detail, maintain a homogenous chemical composition, and behave like a fluid during injection while guaranteeing sufficient wet strength for extraction. The selection of materials in the ceramic core is further limited to those that can be dissolved out using an etchant after casting of the metal blade. Two categories of material are commonly employed: silica and alumina based ceramics [2, 4, 5]. In this work two separate ceramic-wax pastes were considered; one having a higher viscosity, typically injected at higher pressures, the other having a lower viscosity, more suitable for lower pressures and larger cores.

The paste was thermally characterised using several methods: Differential Scanning Calorimetry (DSC) for liquidus and solidus temperatures—Thermal

Gravimetric Analysis (TGA) to assess wax content—laser flash for the thermal diffusivity, and material density using the Archimedes' method.

The flow behaviour of the pastes was characterised using rotational and capillary rheometry, at low and high shear rates respectively. A range of rotational and capillary experiments were carried out from injection temperature to just above the solidification temperature. Yield stress was measured by twin plate rotational rheology, using a stress linear ramp at the injection temperature [6]. All the viscosity readings were fitted using the Herschel-Bulkley model [7] for Bingham plastics limited by a maximum and a minimum viscosity value:

$$\mu(\dot{\gamma}) = \begin{cases} \alpha_T \, \mu_0, & \dot{\gamma} < \frac{\tau_0}{\mu_0} \\ \alpha_T \, \dfrac{\tau_0 + k\left[\alpha_T\left(\dot{\gamma} - \frac{\tau_0}{\mu_0}\right)\right]}{\alpha_T \, \dot{\gamma}}, & \dot{\gamma} \geq \frac{\tau_0}{\mu_0} \end{cases}$$

where μ [Pa s] is the viscosity, $\dot{\gamma}$ [s^{-1}] is the shear rate, α_T the temperature shift factor, τ_0 [Pa] is the yield stress, k the consistency factor and μ_0 [Pa s] the yielding viscosity [8].

The dependence to the temperature is of the Arrhenius' type as follow:

$$\log(\alpha_T) = \frac{E_a}{R}\left(\frac{1}{T} - \frac{1}{T_0}\right)$$

where E_a [J/mol] is the activation energy, $R\left[\frac{\mathrm{J}}{\mathrm{mol\,K}}\right]$ the universal gas constant and T_0 [K] the reference temperature [8].

The computational fluid dynamic (CFD) software environment used was StarCCM+. A fully coupled fluid flow and heat transfer model was created, with physical domains for the dies, fluid volumes, cooling channels, and any additional volumes such as stabilising quartz pins. Regions were meshed using polyhedral elements with multiple prism layers at the walls to capture the heat transfer and high fluid shear rates. A continuous fluid volume was modelled as a Eulerian multiphase problem, with the ceramic paste acting as a liquid phase, and a compressible ideal gas as a secondary phase. Transient simulations were carried out using an implicit unsteady solver, with timestep limited to obtain a target mean value of the Courant-Friedrichs-Lewy number (CFL) of 0.5. The high fidelity of mesh resolution, and small timestep (typically 1e−4), as well as highly viscous fluid meant turbulence was modelled directly, with no additional models required [9]. Gas in the dies was vented at pressure outlets, stopping as soon as obstructed by paste.

The injection parameters used in production were modelled using the defined ramping time and pressure limits. The injection stage comprised of the filling, then the compaction of the material at high pressure; afterwards the injection pressure is removed and the core left to solidify. The cooling and solidification of the core was driven by the large thermal mass of the steel die, with additional cooling channels, which were fully modelled.

Results and Discussion

Simulations of injection and solidification of different die geometries were carried out along with production data analysis. Moreover, two different pastes have been employed depending on the core. Results have been divided by the three highly interacting factors influencing the occurrence of defects after sintering: filling pattern, shear rate, and temperature distribution. The first is highly dependent on the die geometry and the rheology of the paste. The process variable driving the second is the injection speed, while the nozzle temperature and the cooling of the die are responsible for the temperature distribution of the paste.

Filling Pattern

An initial assessment of the material models, boundary conditions and process description was carried out through comparison of simulated injections and real short shots (Fig. 1). The simulations are in excellent agreement with experiments, and are easy to measure using the features on the core, giving confidence in the process description. The material description has also been validated by simulating rheological experiments directly—to be discussed in a later paper.

Short shots are useful to visualise the transient filling pattern, but thanks to modelling it was possible to gather more specific information on the paste such as its residence time and distribution after injection. Figure 2 highlights the injection

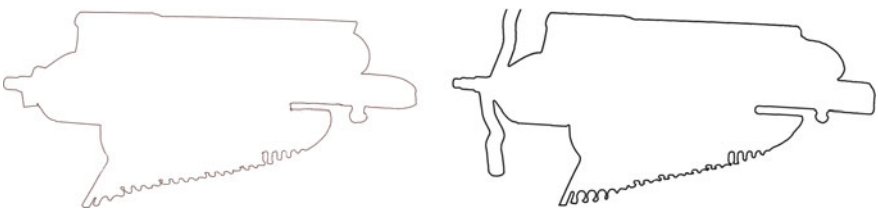

Fig. 1 Outline comparison of a short shot (left) and the simulation (right) at identical injected volume

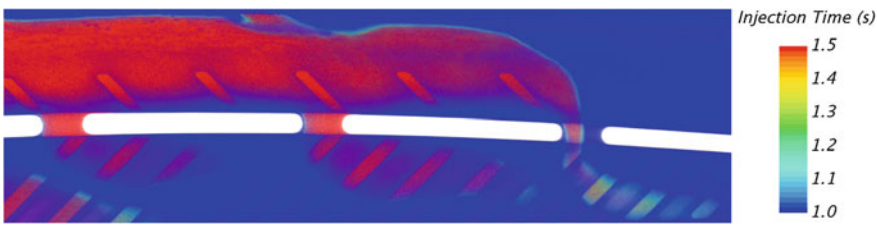

Fig. 2 Turbine blade core detail showing injection time of paste into the mould. Scale highlights the flow of new material into stagnant one

time, showing how streams of newly injected paste interact with the rest of the material. The study of the filling enables prediction of the position of weld lines, to visualise the residence time of the injected paste into the die and highlights crucial information such as stagnant location and feeder efficiency.

The ability of the paste to weld together when two fronts meet is essential in the production of complex shapes. If the temperature of the paste and/or local pressure are not high enough, a weld line will appear, producing a surface defect and an optimal crack initiator [10, 11]. Weld lines are usually identified post injection, with the part scrapped before firing, however, cracks may also be seen post-firing at the meeting point of paste fronts that appeared to have welded together well. The example reported in Fig. 3 demonstrates an area where two fronts meet along an extruded section of the core. Cracks in the fired core, in the location of the simulated meeting fronts are shown. It is common that feeders are under-dimensioned or in a suboptimal location to achieve the required pressure to continuously feed part of the die without stopping, furthermore, long sections with small cross sections are subjected to a higher thermal exchange that the rest of the die, increasing the paste viscosity and therefore the pressure required to weld together. With the merging fronts having a low surface temperature, it seems fair to attribute longitudinal cracks found in this location to such phenomena. As the defect is only detectable post-firing, it is arguable that the two fronts adhered to some degree, but leaving the ceramic particles strongly orientated, so that the stress produced by later shrinkage was released by crack formation.

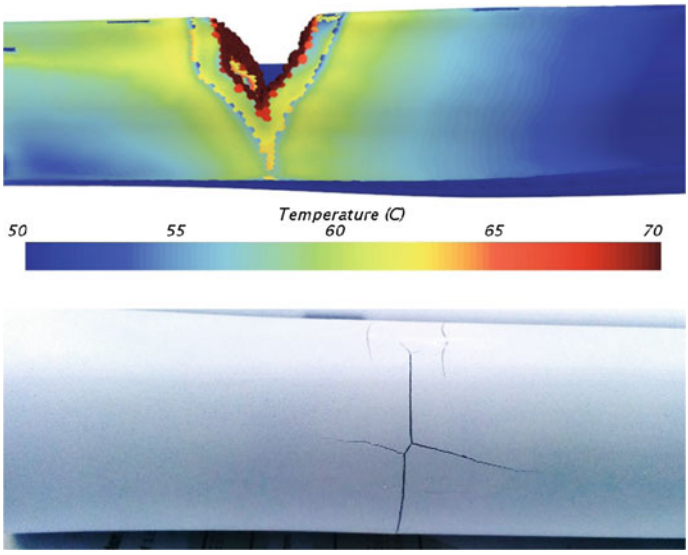

Fig. 3 Top—Simulation showing the last filled volume of a core. Bottom—a post-firing core showing a crack along the weld line

Shear Rates

Temperature, viscosity and instantaneous injection flow rate, in combination with localised die cross-section in the complex geometries typical of technical ceramics determine the velocity and shear rate of the paste. Loaded materials are subjected to phase migration and orientation in areas exhibiting high shear rates [12, 13]. Occurrence of such conditions have been tested by microstructural analysis in different sections and additionally by thermogravimetric investigations on green bodies.

By developing a simple yet useful criterion, recording the maximum shear rate applied to the paste as it moves through the core, the simulation was able to predict the location of cracks recorded after firing of the part. In particular cracks were located where the shear rate was high compared to the surrounding area, suggesting that the geometry variation responsible for the higher local speed has produced a weaker structure (Fig. 4). It is likely that only the liquid phase accommodates the strain by forming particle-free regions away from die walls, where the local speed is higher, whereas particles packed aligned along the walls [14].

Clearly, all of the injected material in the final core will have passed through the inlet, and as such, any poor flow condition here will detrimentally affect the properties of the part. A design modification at the inlet is shown in Fig. 5. The use of conical section from the nozzle to the bulk of the core was optimised through simulation to reduce the maximum shear rate achieved by more than 60%. Furthermore, often such modification can be applied to existing dies. Conical

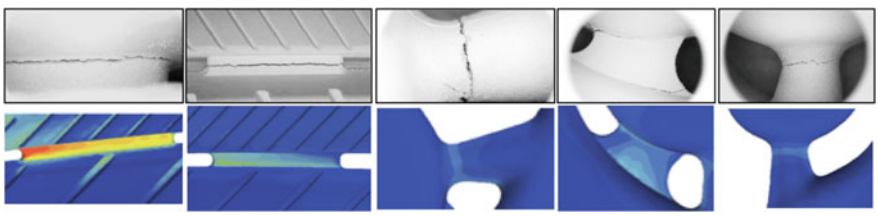

Fig. 4 Localised high values of maximum shear rates and reported post-firing cracks

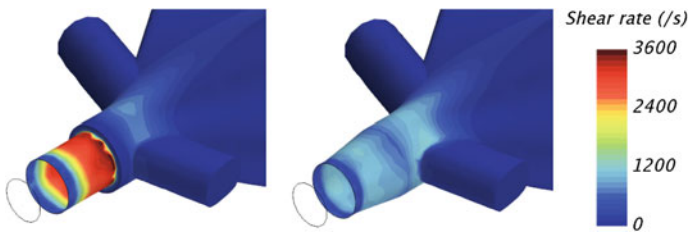

Fig. 5 Shear rate at the inlet using a square section (top) and conical (bottom)

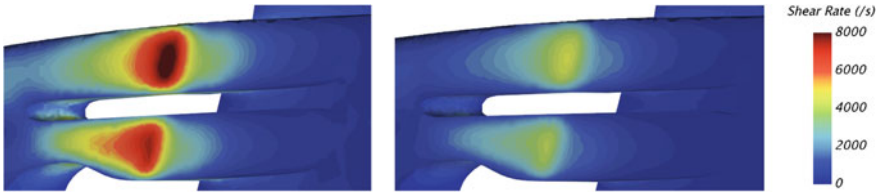

Fig. 6 By changing the flow rate profile of the injection the shear rates achieved in the trailing edge were halved

sections have been reported in a number of investigations [15] to limit the amount of phase migration.

Typical of all blades, high shear rates are found in the trailing edge, as the thinnest section of a core and usually last to fill. In extreme cases, the trailing edge is so thin that the paste velocity increases enough to prevent efficient venting. X-ray radiography has showed the presence of trapped air at the location where stagnant paste in the trailing edge meet with a flux of high velocity new paste. With the ability to simulate the filling, it is possible to modify the injection parameters to reduce the piston or screw speed as the filling front reaches the trailing edge. In this way, the thermal and shear distribution in the bulk of the core is unchanged, with only the last phase of the filling varying. Figure 6 demonstrates a shear rate 50% lower in the most critical section of a core, where most of the defects are located.

Solidification

The thermal conductivity and melting temperature of the pastes simulated were measured. Although CIM solidification has been previously modelled [16, 17] this work also simulated the shape of the water cooling channels within the die, in order to achieve a more representative description of the heat distribution of the tool. It was therefore possible to reproduce the solidification after injection. Other than the formation of weld lines, one of the most severe problems driven by a non-optimal solidification control is the inlet freezing: if the inlet has high thermal losses, it will freeze off prematurely, preventing new injection material to compensate for the solidification shrinkage in the bulk of the core. The resulting ineffective compaction phase leads to internal voids, delamination between the solid skin and the bulk and also weakness on this boundary, due to orientation as reported by other investigations [16, 18, 19]. Figure 7 shows a simulation of a solidifying core, and the isolated liquid phase in the centre of the aerofoil after the inlet has frozen, compared to a picture of the fired core with visible internal lamination.

The primary cause of scrap in our analysis of complex core production is post-firing cracking of the trailing edge, where simulated heat loss predicted the material solidifying along two divergent fronts, pulling the fragile sections apart. In

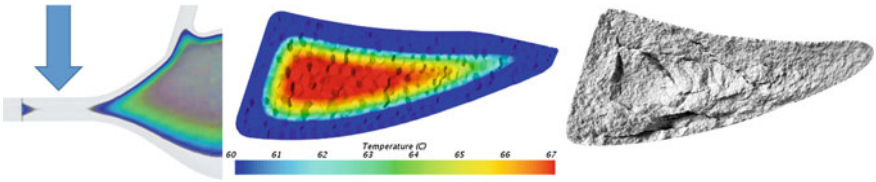

Fig. 7 Left—Molten paste during the compaction phase of the injection, at the point at which the inlet has frozen. Right—a broken core after firing: showing a crack following the perimeter of the part

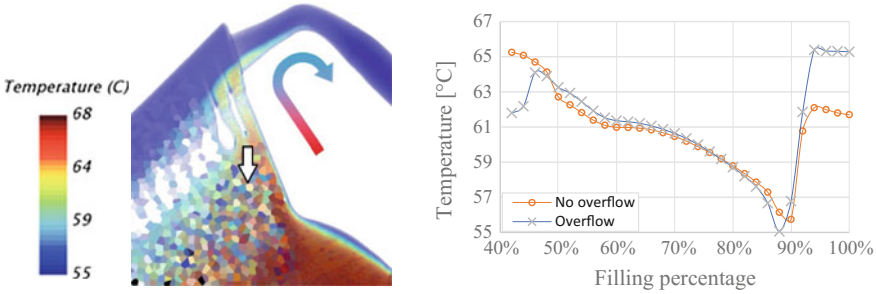

Fig. 8 An additional overflow added to flush through warm paste into critical regions (path of coloured arrow). Graph shows higher temperature achieved with overflow in probe position (white arrow) (Figure censored over critical geometry)

this context, our model was able to provide an insight into the combined flow and solidification results. In particular the die has been modified to have an empty volume next to the trailing edge; this region is partially filled, but remains stagnant during the initial stage of the filling, while the paste flows preferentially into the thickest sections. The empty volume subsequently allows additional, hotter material to flush through the cold, stagnant paste in the last phase of filling, into a non-critical location for the component in Fig. 8. This modification, allowing on average a 5 °C increase in temperature above liquidus has driven an outstanding improvement in production.

Conclusions

In this work filling and solidification of different ceramic cores have been modelled. In particular, results have showed that:

- Cracks form where there are high shear rate gradients
- Weld lines can be eliminated by the use of well-designed feeders and packing stage optimisation

- Injection velocity can be optimised depending on the section being filled
- Die design can be modified to limit phase migration
- Stagnant paste related defects can be overcome by adding sacrificial volumes.

Future work will include the following:

- Building of an experimental system to investigate the severity of weld lines in ceramic pastes at different forming conditions
- Statistical analysis of the production to verify the effect of the die changes made
- Test shots using the proposed injection flow profiles
- Use of an instrumented die to validate further filling and solidification.

In conclusion, by combining accurate description of the process and material behaviour, with an understanding of typical defects formation mechanics this work can be used at the mould design phase to reduce problems often only detectable at the end of the production and reduce design iteration of the die.

Acknowledgements The author gratefully acknowledges financial support from the Centre for Doctoral Training in Innovative Metal Processing (IMPaCT) funded by the UK Engineering and Physical Sciences Research Council (EPSRC), grant reference EP/L016206/1 and Doncasters Group.

A special thanks to Thomas Wright and the Doncasters Technical Centre and to the staff members of the University of Birmingham, in particular Richard Turner, Stuart Blackburn, John Wedderburn and Frank Biddleston.

References

1. Pradyumna R, Baig MAH (2012) Ceramic cores for turbine blades: a tooling perspective. Int J Mech Indus Eng 2(4):1–7
2. Wereszczak AA, Breder K, Ferber MK, Kirkland TP, Payzant EA, Rawn CJ, Krug E, Larocco CL, Pietras RA, Karakus M (2002) Dimensional changes and creep of silica core ceramics used in investment casting of superalloys. J Mat Sci 37(19):4235–4245. doi:https://doi.org/10.1023/A:1020060508311
3. Knight J, William A (2000) Structure property relationships of silica based performed cores for investment casting. Ph.D. thesis, University of Birmingham
4. Wu H, Li D, Tang Y, Sun B, Xu D (2009) Rapid fabrication of alumina-based ceramic cores for gas turbine blades by stereolithography and gelcasting. J Mat Process Technol 209(18–19):5886–5891. doi:https://doi.org/10.1016/j.jmatprotec.2009.07.002
5. Gromada M, Swieca A, Kostecki M, Olszyna A, Cygan R (2015) Ceramic cores for turbine blades via injection moulding. J Mat Process Technol 220:107–112
6. Cheng DCH (1986) Yield stress: a time-dependent property and how to measure it. Rheologica Acta 25(5):542–554. doi:https://doi.org/10.1007/BF01774406
7. Herschel WH, Bulkley R (1926) Measurement of consistency as applied to rubber-benzene solutions. Am Soc Test Proc 26:621
8. STARCCM+ Users Manual. http://www.cd-adapco.com/products/star-ccm/documentation. Accessed 31 Aug 2017
9. Humphreys NJ, McBride D, Shevchenko DM, Croft TN, Withey P, Green NR, Cross M (2013) Modelling and validation: Casting of Al and TiAl alloys in gravity and centrifugal casting processes. Appl Math Model 37(14):7633–7643. doi:https://doi.org/10.1016/j.apm.2013.03.030

10. Hwang J, Choi S, Hong S, Kim N (2013) Determination of the flow stress and thermal properties of ceramic powder feedstock in ceramic injection molding. J Mech Sci Technolo 27(6):1815–1824. doi:https://doi.org/10.1007/s12206-013-0432-0
11. Edirisinghe MJ, Evans JRG (1986) Review: fabrication of engineering ceramics by injection moulding. II. Techniques. Int J High Technol Ceram 2(4):249–278
12. Patel MJ, Wedderburn J, Blackburn S, Wilson DI (2009) Maldistribution of fluids in extrudates. J Eur Ceram Soc 29(5):937–941. doi:https://doi.org/10.1016/j.jeurceramsoc.2008.07.037
13. Barnes EC, Wilson DI, Johns ML (2006) Velocity profiling inside a ram extruder using magnetic resonance (MR) techniques. Chem Eng Sci 61(5):1357–1367
14. Mueller S, Llewellin SW, Mader HM (2009) The rheology of suspensions of solid particles. Kolloid-Zeitschrift 39(4):291–300. https://doi.org/10.1098/rspa.2009.0445
15. Mascia S, Patel MJ, Rough SL, Martin PJ, Wilson DI (2006) Liquid phase migration in the extrusion and squeezing of microcrystalline cellulose pastes. European J Pharm Sci 29(1):22–34
16. Zhang T, Blackburn S, Bridgwater J (1997) Orientation of binders and particles during ceramic injection moulding. J Eur Ceram Soc 2219(96):101–108. doi:https://doi.org/10.1016/S0955-2219(96)00070-2
17. Bilovol VV (2003) Mould filling simulations during powder injection moulding. Delft University of Technology, Netherlands
18. Krug S, Evans JRG, Ter Maat JHH (2002) Differential sintering in ceramic injection moulding: particle orientation effects. J Eur Ceram Soc 22(2):173–181. doi:https://doi.org/10.1016/S0955-2219(01)00259-X
19. Mannschatz A, Muller A, Moritz T, Müller A, Moritz T (2011) Influence of powder morphology on properties of ceramic injection moulding feedstocks. J Eur Ceram Soc 31(14):2551–2558. doi:https://doi.org/10.1016/j.jeurceramsoc.2011.01.013